

RECONSTRUCTION OF LOCALLY FREQUENCY SPARSE NONSTATIONARY SIGNALS FROM RANDOM SAMPLES

Moeness Amin^{*}, *Branka Jokanović*^{*}, and *Traian Dogaru*^{**}

^{*}Center for Advanced Communications, Villanova University, Villanova, PA, USA

^{**}US Army Research Lab, Adelphi, MD 20783, USA

ABSTRACT

The local sparsity property of frequency modulated (FM) signals stems from their instantaneous narrowband characteristics. This enables their reconstruction from few random signal observations over a short-time window. It is shown that for linear FM signals, the sparsity of the local frequencies is equal to the window length, thus adding another specification to the window selection requirements, beside the conventional temporal and spectral resolutions. Stable signal reconstruction within a sliding window depends on the underlying probability distribution function guiding the random sampling intervals. Both simulations and computational EM modeling data are used to demonstrate the effectiveness of local reconstructions. We consider both mono-component FM signals and multi-component signals, corresponding to maneuvering targets and human gait Doppler signatures, respectively.

Index Terms— Local sparsity, nonstationary signals, random under-sampling, time-frequency representation

1. INTRODUCTION

Compressive sensing (CS) has been studied extensively in many areas, including radar [1-5]. In CS, a sparse representation of a signal is projected onto a much lower dimensional measurement space. This leads, in general, to decreasing the data-acquisition requirements from time, logistic, and hardware complexity perspectives. In this regards, it is possible to record a small number of linear measurements of a signal and from those measurements reconstruct the complete set of all samples that can be recorded conventionally [6]. If N is the ambient dimension of the signal, and K is the sparsity level, then the required number of observations, M , is slightly more than K , but far fewer than N .

Nonstationary signals, such as FM signals, are locally sparse, owing to their instantaneous frequency characteristics that render them instantaneously narrowband. However, because of their wideband nature, FM signals are not globally sparse when a large data record is considered, as in the case of spectral analysis of stationary signals [7]. In this paper, we focus on sparsity induced by the small signal local

frequency contents. Reconstruction of a large class of nonstationary signals from few random observations can, therefore, benefit from the sparsity when these signals are only viewed through a short time window. In this case, N represents the total number of time observations, whereas K becomes the number of local multi-component signals. This number may change over different data segments leading to “time-varying” sparsity. The local frequency reconstruction is then poised to outperform global frequency reconstruction for the same frequency grid. Two classes of nonstationary signals are considered:

1) FM signals which are ubiquitous in active sensing using several modalities, including radar, sonar, and ultrasound and are also adopted as interference and jamming signals to intended and non-intended receivers [8-10].

2) MicroDoppler signals which are multi-component that exhibit significant changes in their structures over time. These signals are typically associated with radar returns from vibrating, oscillating, and rotating targets, and they commonly characterize human gait as well as sudden and short gross-motor motions [11-15].

In both classes, we deal with signals as deterministic rather than nonstationary random processes [16]. This paper differs from other recently published work on sparse reconstruction using quadratic time-frequency signal representations [17-21]. Our contribution underlines the role of the sliding windows in the CS paradigm for nonstationary signals. Preprocessing of these signals for the purpose of stationarization prior to reconstruction is not considered. Rather, we use a short-time window which determines the level of sparsity and represents another specification that adds to the window temporal and spectral resolution requirements. For a chirp signal, the window length becomes equal to the corresponding local frequency sparsity captured within the window’s boundaries. Among possible models of random sampling [22], we consider the special case where the window length is longer than the maximum possible sampling interval. In this case, increasing the window length would reduce sparsity, but the average sampling frequency remains the same.

Section 2 in this paper discusses local sparsity, whereas Section 3 includes window analysis and sparse reconstructions. Section 4 demonstrates, by simulations, local sparse

reconstructions of both FM and micro Doppler signals using Orthogonal Matching Pursuit (OMP) technique.

2. LOCAL SIGNAL SPARSITY

An *ideal* time-frequency representation of a single FM signal shows:

1) Sparsity in the two-dimensional (2D) time-frequency (TF) domain by the virtue of perfect power localization of FM signals, making it appear as a wavy line in a plane populated by zero values. As such, for a single FM component, the joint-variable TF representation is N -sparse.

2) Local frequency sparsity, where the intersection of a vertical time slice and the wavy line produces only one non-zero value over frequency. This, in turn, establishes a $K=1$ sparsity property.

3) Time sparsity along a frequency slice where there is typically one or few nonzero values along the time variable, which amounts to K equals to, or slightly greater than one.

The above three cases of sparsity are depicted in Fig. 1 using a sinusoidal FM signal as an example. For multi-component signals, where each component is defined by a frequency law, there would be more intersections points, leading to reduced sparsity compared to the single component FM case. This is also illustrated in Fig. 1 with a chirp signal added to the sinusoidal FM.

With non-ideal representations, the time and frequency slices are, respectively, replaced by short windows and narrowband filters, as depicted in Fig 2. In this case, sparsity is again reduced compared to the ideal case, due to the inclusion of consecutive time or frequency points. For micro-Doppler signals, corresponding to human gross-motion activities, the frequency support of local sparsity has more than one frequency occupancy. The number and locations of those values may vary with the short time segment analyzed, with K typically exceeding one over most time segments. We focus in this paper on local frequency sparsity for different classes of signals using non-ideal representation, i.e., pursue short-time sliding window analysis and local frequency reconstruction.

3. LOCALLY SPARSE TIME-FREQUENCY REPRESENTATION

To exploit the nonstationary signal local sparsity, we partition the data into overlapping segments and carry signal reconstruction over each segment separately. Let \mathbf{d}_n denote the reconstructed frequency representation corresponding to time n , $n \in [1, N]$. This reconstruction can be written as the following optimization problem [23],

$$\begin{aligned} & \text{minimize } \|\mathbf{d}_n\|_1 \\ & \text{subject to } \mathbf{y}_n = \mathbf{A}_n \mathbf{d}_n \end{aligned} \quad (1)$$

where \mathbf{y}_n is the windowed-observation vector, while matrix \mathbf{A}_n represents a partial Fourier matrix.

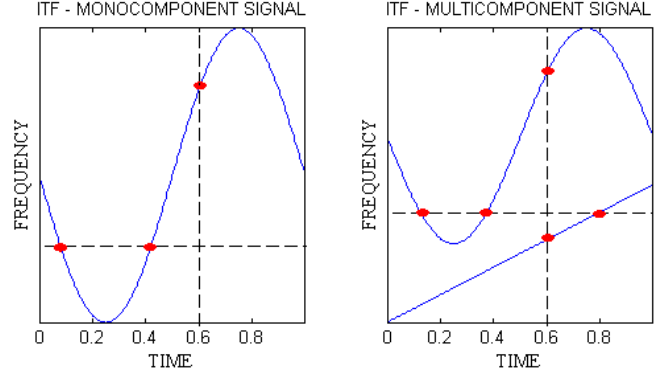


Fig. 1. Ideal time-frequency representation for given mono-component and multi-component signals.

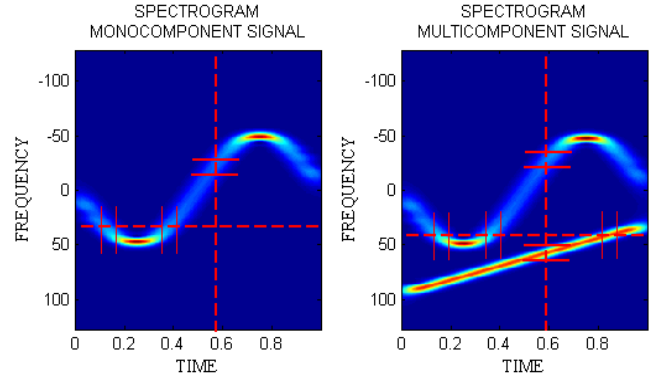


Fig. 2. Spectrogram for given mono-component and multi-component signals.

The rows of \mathbf{A}_n are drawn from the rows of the N -dimensional discrete Fourier transform (DFT) matrix. In this sense, it is an overcomplete dictionary with the matrix columns representing a redundant DFT frame. The solution of (1) can provide one form of sparse time-frequency representation (SPTFR) \mathbf{D} as,

$$\mathbf{D} = [\mathbf{d}_1, \dots, \mathbf{d}_N]. \quad (2)$$

It is important to note that the SPTFR is different from the short-time Fourier transform (STFT), and its magnitude square is not the Spectrograms. We use OMP algorithm for reconstruction, motivated by its suitability for large-scale applications.

3.1. Sparsity level for mono-component signals

We consider a class of chirps which are an important member of FM signals. The slope in time-frequency plane is determined by the chirp rate. For a signal of the form,

$$x(t) = Be^{jat^2/2}, \quad (3)$$

the extent of the local frequency band, W , and therefore sparsity level, consists of all instantaneous frequencies captured by the window. These frequencies are determined by the window length T and the chirp rate a . For uniformly sampled discrete signals, the local frequency sparsity, which

represents the number of grid frequencies spanning the local frequency band, becomes

$$K = \frac{aT_s N_w}{\Delta\omega}, \quad (4)$$

where T_s is sampling period, $\Delta\omega$ defines the frequency grid density, and N_w is the window length in samples. The frequency grid defines the desired resolution and, as such, is assumed fixed, independent of the window length. It is noted that a reasonable choice of this grid spacing is the minimum frequency resolution achieved through Nyquist sampling of the entire signal. For the underlying class of chirp signals, the frequency spacing is given by

$$\Delta\omega = aT_s. \quad (5)$$

Accordingly

$$K = N_w, \quad (6)$$

which simply means that *the sparsity level is defined by the window length*. The minimum number of local observations, M , needed for windowed chirp reconstruction can be obtained through the well-known formula, relating N , M , K and some positive constant c [20],

$$M \geq cN_w \log N. \quad (7)$$

Note that in the above formula, M represents the number of measurements within one window.

For piecewise chirp signals or other mono-component signals different from linear FM, the sparsity within a window could be time-varying and depends on the sliding window position. For this case, one simple option is to estimate the maximum instantaneous bandwidth and then, proceed with the reconstruction using the window size and number of OMP iterations corresponding to this minimum sparsity. Another method, although more computationally demanding, is to adapt window size and number of iterations for each time instant.

A specific case arises if we consider the ratio, β , of the missing samples to the total number N to be known, and if we assume that this ratio is preserved within each window, then the number of measurements within one window is given by,

$$M = (1 - \beta)N_w. \quad (8)$$

One structured sampling scheme satisfying (8) is to select M observations for the initial window position and then add either zero or a new observation as we shift the window one sample so as to maintain the ration fixed. According to (7) and (8), in order to have a successful chirp reconstruction, the percentage of samples available should satisfy the following relation:

$$1 - \beta \geq c \log N \quad (9)$$

Equation (9) can be put in context based on the random sampling interval and its probability distribution function $P(\tau_n = nT_s)$. Only multiple integer n of the Nyquist sampling period is applied. In [22], several distributions of sampling intervals were considered for aliasing noise floor analyses,

including exponential, uniform, geometric and binomial. Each of those distributions influences the choice of the appropriate window size, and can be examined separately. Expression (9) represents a specific realization in which the window includes the maximum possible sampling interval. This renders the average sampling interval fixed within the window, irrespective of increased window size. In radar applications, this would amount to using a window length equal to or longer than any of the staggering pulse repetition periods. If we denote the maximum sampling interval as τ_{max} , then

$$E[\tau_n(N_w)] = \tau_{ave} < \tau_{max}, \quad (10)$$

where τ_{ave} is the averaging sampling interval expressed as a function of window size. In this class of random sampling distributions, the condition for reconstruction becomes independent of the window size.

4. SIMULATIONS

This section demonstrates the performance of global and local reconstructions when applied to different types of signals. Global reconstruction is performed to produce SPTFR over the entire data record. We consider chirps and human gait microDoppler as representatives of mono-component and multi-component signals, respectively. In order to verify the proposed approach, the data is first sampled uniformly at Nyquist rate, and then thinned by discarding some of the samples. When computing TF signal representation, Hanning window is used.

In the first example, we perform local reconstructions of chirp signal when 50% of Nyquistly sampled data are missing randomly. Chirp signal is of the following form

$$x(n) = e^{j64\pi n^2} \text{ where } |n| \leq 1.$$

The number of OMP iterations for local reconstruction is set equal to the window size, $N_w=32$, whereas for global reconstruction, we use the total signal length, $N=256$. The results are depicted in Fig. 3, and demonstrate the expected failure of global reconstruction due to the lack of sparsity. The local reconstructions for different window sizes are shown in Fig. 4. We can observe that the window size plays an important role in the reconstruction process. Increasing the window length compromises the assumption that signal is sufficiently sparse within the window, and as such yields improper and unstable reconstruction. Also, we include results corresponding to different percentages of Nyquist samples, namely from 10% to 90%. As a measure of successful reconstruction, we use structural similarity index [24]. This index measures the similarity between two images. The maximum index value 1 corresponds to the case when two images are identical. We use the result when there are no missing samples as a reference image and compare it with the SPTFR. The results for different window sizes are shown in Fig. 5.

The following remarks are in order:

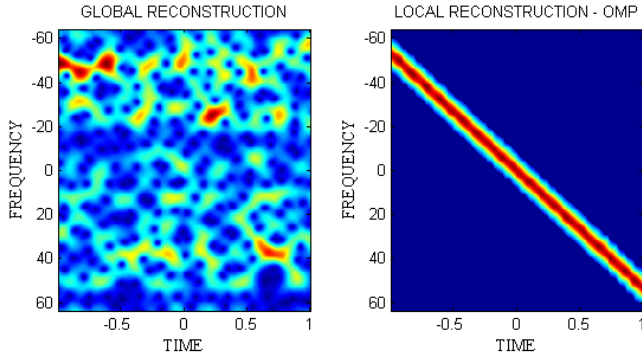


Fig. 3. Global and local reconstruction of chirp signal when 50% of data is missing

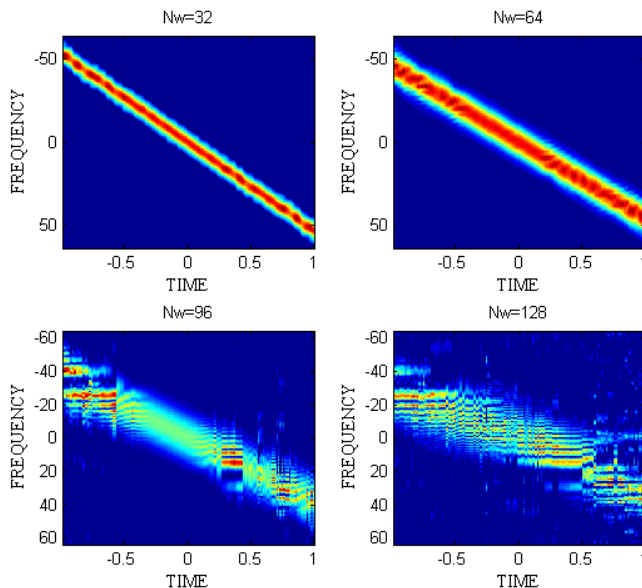


Fig. 4. Local reconstruction of chirp signal for different window widths: $N_w=32$, $N_w=64$, $N_w=96$, $N_w=128$. 50% of data is missing.

- 1) For few missing samples, the window size is irrelevant to performance;
- 2) Large size windows, such as $N_w=96$, 128, capture corresponding large sub-bands, making K assume very high values and producing inferior results to their small size windows counterparts ($N_w=32$, 64).

In the next example, we consider computational EM modeling data corresponding to a human walking straight toward a pulse-Doppler radar (which means 0° azimuth). Vertical polarization is considered. The radar operates around 1 GHz, with a bandwidth is 80 MHz. Also, we consider a walking cycle takes 2 seconds. The EM solver, Finite Difference Time Domain (FDTD) is used. Reference [25] includes more information on the data modeling generation. This modeling data differs from the experimental data used in [21], where the latter deliberately emphasized the arms more than the leg movements. We randomly remove 45% of data. Fig. 6 shows that global reconstruction fails once again to depict the torso and limbs movements.

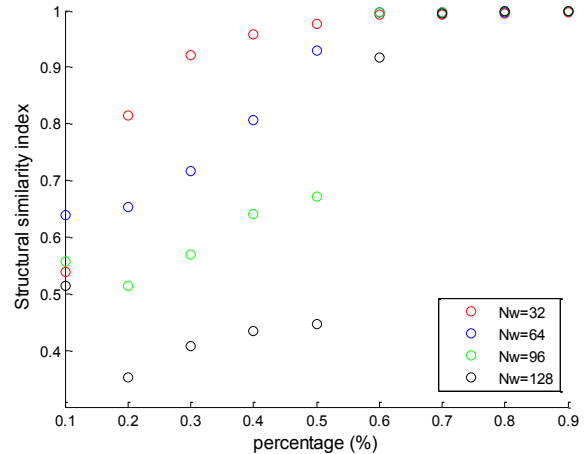


Fig. 5. Structural similarity index for the results using different window widths N_w and different percentage of present samples.

The local reconstruction resembles the Spectrograms with all uniformly sampled data available. This resemblance will lend itself to proper motion classifications under missing or random observations.

5. CONCLUSION

In this paper, compressive sensing is used to reconstruct the signal local frequencies, and thus provides the time-frequency signatures of mono- and multi-component nonstationary signals. The proposed approach is based on the reconstruction of data within short overlapping time intervals defined by a sliding window. It was shown that the sparsity level is dependent on the applied window and is equal to its length when a chirp signal is considered. The paradigm of sparsity, number of observations, and window length was discussed and demonstrated by simulations and EM modeling examples involving both FM signals and human gait microDoppler radar returns.

6. REFERENCES

- [1] R. Baraniuk and P. Steeghs, "Compressive radar imaging," in *Proc. IEEE Radar Conf.*, Waltham, MA, 2007, pp.128-133.
- [2] M. Herman and T. Strohmer, "High-resolution radar via compressive sensing," *IEEE Trans. Signal Process.*, vol. 57, no. 6, pp. 2275-2284, 2009.
- [3] J. G. Ender, "On compressive sensing applied to radar," *Signal Process.*, vol. 90, pp. 1402-1414, 2010.
- [4] M. Amin and F. Ahmad, "Compressive Sensing for through the wall radar imaging," *J. of Electron. Imaging*, vol. 22(3), Jul-Sep 2013.
- [5] M. Amin, Ed., *Compressive sensing for urban radar*, CRC Press, 2014.
- [6] M. Davenport, P. Boufounos, M. Wakin and R. Baraniuk, "Signal processing with compressive measurements," *IEEE J. Sel. Topics Signal Process.*, vol. 4, no. 2, pp. 445-460, 2010.

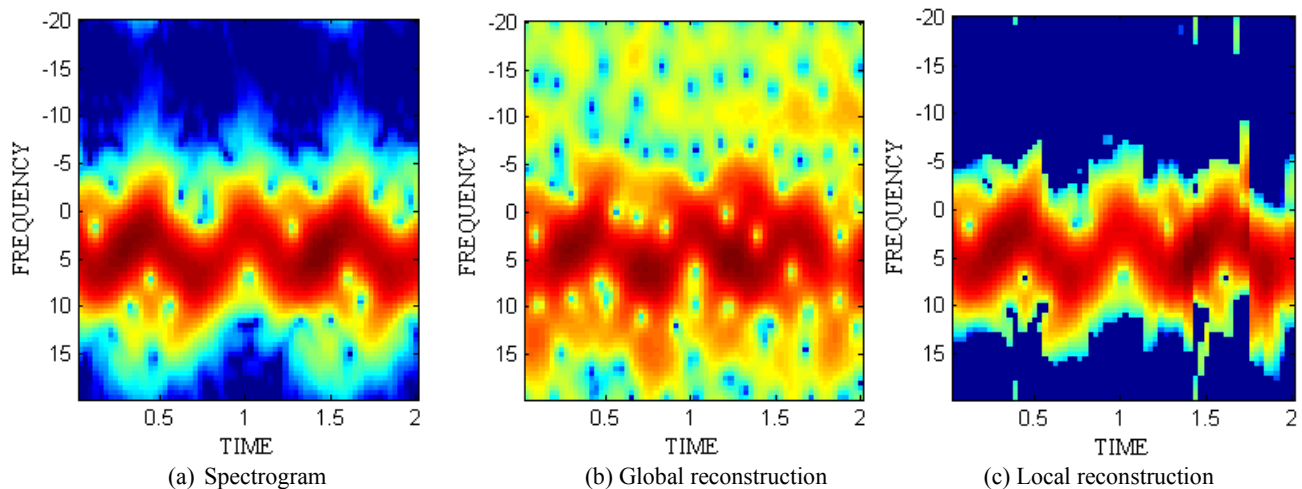


Fig. 6. (a) Spectrogram obtained from data with no missing samples; (b) Global reconstruction; (c) Local reconstruction of human gait signal when 45% of data is missing.

- [7] M. F. Duarte, and R. G. Baraniuk, "Spectral compressive sensing," *Appl. and Computational Harmonic Anal.* 35, no. 1, pp. 111-129, 2013.
- [8] W. C. Knight, R. G. Pridham, and S. M. Kay, "Digital signal processing for sonar," in *Proc. IEEE*, vol. 69, issue 11, pp.1451-1506, 1981.
- [9] M. Amin, L. Zhao, and A. Lindsey, "Subspace array processing for the suppression of FM jamming in GPS receivers," *IEEE Trans. Aerosp. Electron. Syst.*, vol. 40, no. 1, pp. 80-92, 2004.
- [10] T. Misaridis and J. A. Jensen, "Use of modulated excitation signals in medical ultrasound. Part I: basic concepts and expected benefits," *IEEE Trans. Ultrason., Ferroelectr., Freq. Control*, vol. 52, no. 2, 2005.
- [11] C. Clemente, A. Balleri, K. Woodbridge, and J. Soraghan, "Developments in target micro-Doppler signatures analysis: radar imaging, ultrasound and through-the-wall radar," *EURASIP J. Adv. Signal Process.*, 2013.
- [12] V. C. Chen, "Analysis of radar micro-Doppler signature with time-frequency transform," in *Proc. 10th IEEE Workshop Stat. Signal and Array Process. (SSAP)*, Pocono Manor, Pa, 463-466, August 2000.
- [13] P. Setlur, M. G. Amin, and F. Ahmad, "Analysis of micro-Doppler signals using linear FM basis decomposition," in *Proc. SPIE*, vol. 6210, May 2006.
- [14] Y. Kim, and H. Ling, "Human Activity Classification Based on Micro-Doppler Signatures Using a Support Vector Machine," *IEEE Trans. Geosci. Remote Sens.*, vol. 47, no. 5, pp. 1328 – 1337, 2009.
- [15] F. Ahmad, M. G. Amin, and P. Setlur, "Through-the-wall target localization using dual-frequency CW radars," in *Proc. of SPIE*, vol. 6201, May 2006.
- [16] M. G. Amin, "Time-frequency spectrum analysis and estimation for nonstationary random processes," in *Time-Frequency Signal Analysis: Methods and Applications*, Ed., B. Boashash, Longman Cheshire, 1992.
- [17] P. Flandrin, and P. Borgnat, "Time-frequency energy distributions meet Compressed Sensing," *IEEE Trans. Signal Process.*, vol. 58, no. 6, 2010.
- [18] LJ. Stankovic, S. Stankovic, I. Orovic, and M. G. Amin, "Robust time-frequency analysis based on the L-estimation and compressive sensing," *IEEE Signal Process. Lett.*, vol. 20, no. 5, pp. 499-502, May 2013.
- [19] LJ. Stankovic, I. Orovic, S. Stankovic, and M. G. Amin, "Compressive sensing based separation of non-stationary and stationary signals overlapping in time-frequency," *IEEE Trans. Signal Process.*, vol. 61, no. 18, pp. 4562-4572, Sept. 2013.
- [20] Y. D. Zhang, M. G. Amin, and B. Himed, "Reduced interference time-frequency representations and sparse reconstruction of undersampled data," in *Proc. Signal Process. Conf. (EUSIPCO)*, Marrakech, Morocco, Sept. 2013.
- [21] B. Jokanović, M. G. Amin, and S. Stanković, "Instantaneous frequency and time-frequency signature estimation using compressive sensing," in *Proc. SPIE*, vol. 8714, May 2013.
- [22] L. Chenchì and J. McClellan, "Discrete random sampling theory," in *Proc. ICASSP*, Vancouver, B. C, Canada, May 2013, pp.5430-5434.
- [23] E. J. Candes, J. Romberg, and T. Tao, "Robust uncertainty principles: exact signal reconstruction from highly incomplete frequency information," *IEEE Trans. Inf. Theory*, vol.52, no.2, pp.489-509, Feb. 2006.
- [24] Z. Wang, A. C. Bovik, H. R. Sheikh, and E. P. Simoncelli, "Image quality assessment: from error visibility to structural similarity," *IEEE Trans. Image Process*, vol.13, no.4, pp.600-612, Apr. 2004.
- [25] T. Dogaru, C. Le, and G. Kirose, "Analysis of the Radar Doppler Signature of a Moving Human," *U.S. Army Research Laboratory, Tech. Report*, 2004.